https://doi.org/10.5194/esd-2022-37
Preprint. Discussion started: 1 August 2022

Earth System Dynamics Discussions

Reconstructions and predictions of the global carbon budget with an emission-driven Earth System Model

Hongmei Li[1], Tatiana Ilyina[1], Tammas Loughran[2*], Aaron Spring[1], and Julia Pongratz[2]

[1]Max Planck Institute for Meteorology, Hamburg, Germany
[2]Department of Geography, Ludwig-Maximilians-Universität, Munich, Germany
[*]Now at CSIRO Oceans and Atmosphere, Aspendale, Victoria, Australia

Correspondence: Hongmei Li (hongmei.li@mpimet.mpg.de)

Abstract. The global carbon budget (GCB) - including fluxes of CO_2 between atmosphere, land and ocean, and its atmospheric growth rate - show large interannual to decadal variations. Reconstructing and predicting the variable GCB is essential for tracing the fate of carbon and understanding the global carbon cycle in the changing climate. We use a novel approach to reconstruct and predict the next-years' variations in GCB based on our decadal prediction system enhanced with an interactive carbon cycle. By assimilating physical atmospheric and oceanic data products into the Max Planck Institute Earth system model (MPI-ESM), we can well reproduce the annual mean historical GCB variations from 1970-2018, with high correlations relative to the assessments from the Global Carbon Project of 0.75, 0.75 and 0.97 for atmospheric CO_2 growth, air-land CO_2 fluxes and air-sea CO_2 fluxes, respectively. Such a fully coupled decadal prediction system, with an interactive carbon cycle enables representation of the GCB within a closed Earth system, and therefore provides an additional line of evidence for the ongoing assessments of the anthropogenic GCB. Retrospective predictions initialized from the assimilation simulation show high confidence in predicting the following year's GCB. The predictive skill is up to 5 years for the air-sea CO_2 fluxes, and 2 years for the air-land CO_2 fluxes and atmospheric carbon growth rate. This is the first study investigating the GCB variations and predictions with an emission-driven prediction system, such a system also enables the reconstruction and prediction of the evolution of atmospheric CO_2 concentration changes. The earth system predictions in this study provide valuable inputs for understanding the global carbon cycle and informing climate relevant policy.

1 Introduction

The CO_2 fluxes between the atmosphere, land and ocean, and thus the atmospheric carbon growth rate, vary substantially on interannual to decadal time-scales (Peters et al., 2017; Friedlingstein et al., 2019; Landschützer et al., 2019; Friedlingstein et al., 2020). These variations reflect combined effects of internal variability of the global carbon cycle (Li and Ilyina, 2018; Séférian et al., 2018; Spring et al., 2020; Fransner et al., 2020) and its responses to external forcings (McKinley et al., 2020).

https://doi.org/10.5194/esd-2022-37
Preprint. Discussion started: 1 August 2022

Earth System Dynamics Discussions

To constrain the global carbon budget (GCB) of the past and facilitate its prediction and projection into the future, the Global Carbon Project (Canadell et al., 2007) assesses the anthropogenic GCB - i.e., CO_2 emissions and their redistribution among the atmosphere, ocean, and land - every year since 2007. The annual updates of the GCB are important in informing policy/society on the ongoing variations in the carbon cycle and will be critical in decarbonization processes. This assessment is based on anthropogenic CO_2 emissions, observations of the atmospheric CO_2 concentration, and individual stand-alone model simulations of CO_2 fluxes for the ocean and land. The air-land CO_2 fluxes from earth system models are the sum of natural fluxes and the land-use change induced emissions, and hence the GCBs use a separate bookkeeping approach (e.g. Hansis et al. (2015)) to calculate only the land-use emissions term. The stand-alone simulations for the land and ocean are forced by different observation/reanalysis data and thus do not provide an internally consistent estimate of the CO_2 fluxes. Moreover, the accumulated CO_2 fluxes from these stand-alone model simulations do not exactly match the observations. Therefore, the global carbon budget is not closed but ends up with a budget imbalance term up to 2 PgC/year for some years (Friedlingstein et al., 2020), which hinders full attribution of the global carbon cycle variations. A large part of the budget imbalance could also be attributed to the mismatch of net biome production between the dynamic global vegetation models (DGVMs) used in the GCBs and inversions that match the atmospheric CO_2 growth rate (Bastos et al., 2020).

Reconstruction of the variable GCB within a closed Earth system model (ESM) is of essential value of tracing the fate of carbon. In addition to assessing the GCB variations in the past, the Global Carbon Project also makes a prediction of the GCB for the next year, however, it is only based on statistical approaches, which is not possible to trace back to the processes. The decadal prediction systems based on ESMs (Marotzke et al., 2016) show potential to reconstruct and predict the global carbon cycle (Li et al., 2016; Spring and Ilyina, 2020). By assimilating observational products of physical fields, the decadal prediction systems are able to reproduce the variations of CO_2 fluxes as found in observation-based products; decadal prediction systems can then use states from an assimilation simulation as initial conditions for further multi-year predictions of the global carbon cycle (Li et al., 2016, 2019; Lovenduski et al., 2019b, a; Ilyina et al., 2021). However, as of now, the state-of-the-art decadal prediction systems are typically forced with prescribed atmospheric CO_2 concentration without an interactive carbon cycle, i.e., CO_2 fluxes are not reflected in the atmospheric CO_2 variations. With this conventional model setup, one can only assess the CO_2 fluxes into the land and ocean, but not the resulting variations in atmospheric CO_2 concentration and growth.

Prediction systems have proven skill in predicting air-sea and air-land CO_2 fluxes (Ilyina et al., 2021), for the first time, we extend our previously concentration-driven prediction system to an emission-driven system, taking into account the interactive carbon cycle and hence resolving prognostic atmospheric CO_2 and making atmospheric CO_2 predictions. In this study, we assess the global carbon budget in a simulation with assimilated observational products into the model, and further estimate the predictive skill based on the Max Planck Institute Earth system model (MPI-ESM) relative to the GCB from 2019 (GCB2019, Friedlingstein et al. (2019)) CO_2 fluxes and atmospheric CO_2 (Dlugokencky and Tans, 2020).

The assimilation simulation is designed to reconstruct the evolution of the earth system of the real world, by incorporating essential fields from observational products into the MPI-ESM. The reconstruction from the fully coupled model simulation (henceforth known as simply the assimilation simulation) enables representation of the global carbon budget within a closed Earth system. Therefore, by construction, this approach avoids the budget imbalance term arising from the need to budget

https://doi.org/10.5194/esd-2022-37
Preprint. Discussion started: 1 August 2022

Earth System Dynamics
Discussions

carbon fluxes from stand-alone models and observations. Our reconstructions of the carbon budget provide an additional and novel estimate. The assimilation simulation states, which are close to the real world, are then used to start our retrospective initialized prediction simulations to predict the changes of the global carbon budget in the next years. Initialized predictions are expected to capture internal variability better than freely evolving uninitialized simulations due to the improved initial conditions. In prediction studies, the "uninitialized" refers to not initialized from states constrained by observations or data products. This novel prediction will be added to enhance robustness of the coming GCB assessment of the Global Carbon Project.

2 Materials and Methods

2.1 Model and simulations

We use the MPI-ESM1.2-LR (Mauritsen et al., 2019), which is the low resolution version used for the sixth phase of the Coupled Model Intercomparison Project (CMIP6). The atmospheric horizontal resolution has a spectral truncation at T63 or approximately 200-km grid spacing with 47 vertical levels. The resolution of the ocean model MPIOM (Marsland et al., 2003) is about 150 km with 40 vertical levels. The ocean biogeochemistry component of MPI-ESM is represented by HAMOCC (Ilyina et al., 2013; Paulsen et al., 2017), and the land and vegetation component is represented by JSBACH (Reick et al., 2021).

Similar to our previous prediction system (Li et al., 2016, 2019), we performed 3 sets of simulations (see Table S1): (i) uninitialized freely evolving historical simulations, (ii) an assimilation simulation performed by nudging the observational signal of climate variations into the model, and (iii) initialized simulations (also referred to as hindcasts or retrospective predictions) starting from states of the assimilation simulation, to investigate the capacity of our model to reconstruct and predict the global carbon budget. The assimilation run is needed for the initialized prediction simulations, and the uninitialized simulations are references to compare to and assess the improved predictability due to initialization.

The major difference relative to the previous system (Li et al., 2016, 2019) is that the new prediction system is based on emission-driven simulations, which are forced by CO_2 emissions instead of prescribed atmospheric CO_2 concentration. In this way, the atmospheric CO_2 concentration evolves in response to the interaction with the strength in CO_2 uptake/outgassing of the land and ocean. We use the CMIP6 (Eyring et al., 2016) historical emissions forcing for our simulations and for extension simulations to 2099 we use the emissions from the SSP2-4.5 scenario (Jones et al., 2016). While the fossil fuel emissions are prescribed, the land-use change induced emissions are prognostic in the ESMs and driven with the Land-Use Harmonization (LUH2) forcing (Hurtt et al., 2020). We use transient land use transitions rather than land-use states and include natural disturbances with dynamic vegetation (Reick et al., 2021). An ensemble of 10 members is run for the uninitialized historical and initialized prediction simulations. The uninitialized ensembles are generated by starting from different year of the control simulation (the model has reached equilibrium as shown in the time series of ocean net primary production and CO_2 fluxes from the control simulation in Fig. A1). The initialized ensembles are generated with lagged 1-day initializations from a given branching point of the assimilation simulation. Note that the initialized 5-year long predictions start annually from November

https://doi.org/10.5194/esd-2022-37
Preprint. Discussion started: 1 August 2022

Earth System Dynamics
Discussions

1st for the period 1960-2018. Fig. 1 illustrates the evolution of atmospheric carbon growth rate in uninitialized, assimilation and initialized simulations. More details of the simulations are summarized in Table A1.

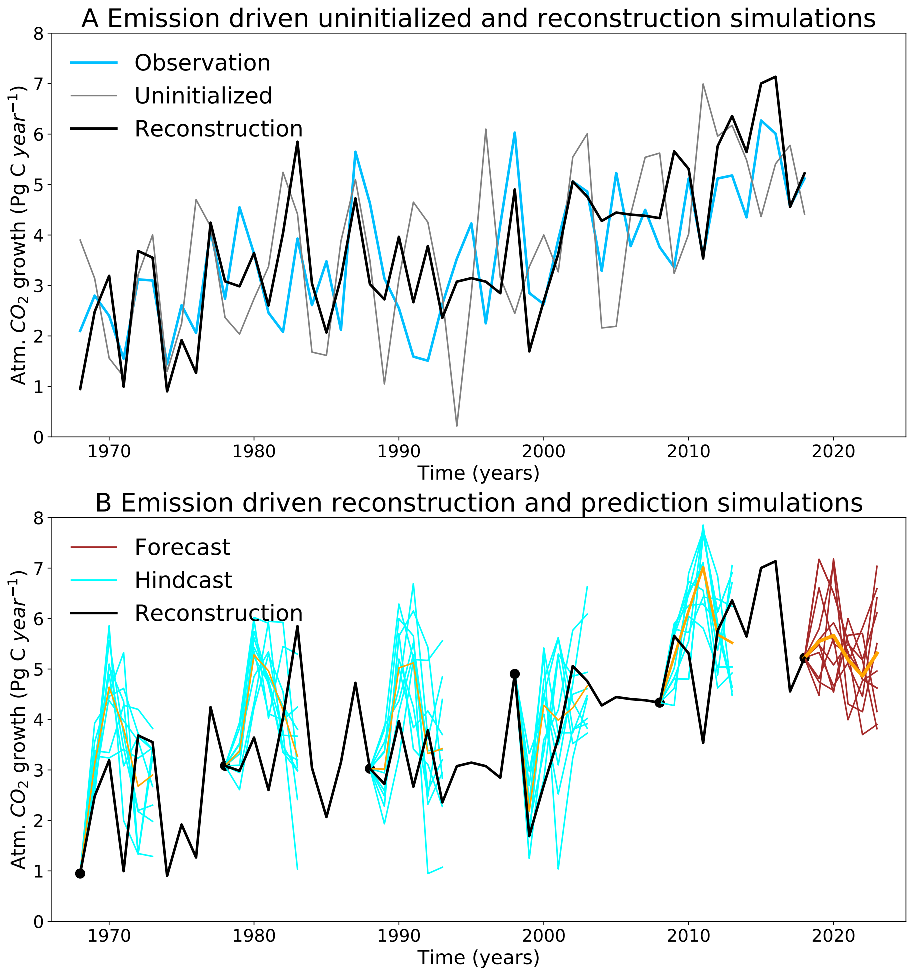

Figure 1. Sketch plot of reconstruction and prediction of the atmospheric CO_2 growth rate. The time series are original model outputs on annual mean frequency. The upper panel plot A, time series show that the assimilation simulation forces the variations in the uninitialized freely run simulation towards the observation (GCB data) and results in a reconstruction close to the data. The lower panel plot B presents the reconstruction together with 5-year long hindcasts and forecasts. To make the illustration clearly, only starting years at 10 year intervals are shown.

2.2 Assimilation methods

Similar to our previous concentration-driven decadal prediction systems (Li et al., 2019), the assimilation is done with nudging the ocean 3-D temperature and salinity anomalies from the ECMWF ocean reanalysis system 4 (ORAS4) (Balmaseda

https://doi.org/10.5194/esd-2022-37
Preprint. Discussion started: 1 August 2022

Earth System Dynamics
Discussions

et al., 2013) and the atmospheric 3-D full-field temperature, vorticity, divergence, and log surface pressure from ECMWF Re-Analysis ERA40 (Uppala et al., 2005) during the period 1960-1979 and ERA-Interim (Dee et al., 2011) during the period 1980-2018. The sea-ice concentration is nudged towards the National Snow and Ice Data Center (NSIDC) satellite observations (as described in Bunzel et al. (2016)). The nudging is applied to every model time step but with different relaxation time, i.e., a relative longer relaxation time of 10 days for the ocean temperature and salinity, and a shorter relaxation time of 6 hours, 24 hours and 48 hours for the atmospheric vorticity, temperature and pressure, and divergence, respectively. The chosen variables for assimilation and the respective relaxation time are according to previous investigations of decadal climate prediction based on MPI-ESM (Marotzke et al., 2016). Direct assimilation of the carbon cycle related variables is not included because of the limited available data; instead, we found that the global carbon cycle is well represented from the assimilation of physical variables only (Li et al., 2016, 2019; Lovenduski et al., 2019b, a; Ilyina et al., 2021), and furthermore, a recent study based on a perfect-model framework (i.e., based on simulations in which the model tries to predict itself) revealed that direct assimilation of the global carbon cycle only brings trivial improvement of predictive skill of the global carbon cycle (Spring et al., 2021). To avoid spurious upwelling in the equatorial region caused by assimilation (Park et al., 2018), we exclude the equatorial band of 5°S-5°N from nudging ocean data.

2.3 Carbon budget decomposition with CBALONE simulations

The GCB from Global Carbon Project is decomposed into 5 terms plus an imbalance term: the two emissions terms from fossil-fuel and land-use changes, and the three sink terms for the natural terrestrial sink, ocean sink, and atmospheric growth on annual timescale. The fossil fuel emissions are prescribed as forcing, and terrestrial and ocean carbon sinks and atmospheric growth terms can be directly derived from the ESM. However, only the net land-atmosphere exchange is directly deducible from an ESM, which is the sum of land-use change emissions and the natural terrestrial sink. In order to separate the two land-related fluxes, we use a stand-alone component of JSBACH called CBALONE as a diagnostic for a direct comparison with the land-use terms from the Global Carbon Project (Friedlingstein et al., 2019). CBALONE is forced by the MPI-ESM daily outputs including 2m air temperature, soil temperature, precipitation, net primary productivity (NPP) per plant functional type (PFT), leaf area index (also per PFT), and maximum wind. We run two parallel simulations, i.e., one with anthropogenic land use changes and another without those changes, comparison of the two simulations differentiate the land-use change induced emissions from the land sink. More details of the method on separating the land-use change induced emission can be found in Loughran et al. (2021).

2.4 Predictive skill quantification

The focus of the study is on global mean variations in atmosphere CO_2 and globally integrated air-sea and air-land CO_2 fluxes on annual timescale. The initialized simulations are investigated according to their lead time, i.e., how many model years they have been integrated freely after restarting from the assimilation simulation. The time series of initialized simulations at lead time of 1 year (2, 3, 4, and 5 years) combine the 1st year (2nd, 3rd, 4th, and 5th year) predictions from initialized simulations of all the starting years from 1959-2018, therefore, the time series at lead time of 1 year (2, 3, 4, and 5 years) are from 1960-2019

https://doi.org/10.5194/esd-2022-37
Preprint. Discussion started: 1 August 2022

(1961-2020, 1962-2021, 1963-2022, and 1964-2023). The analyses of predictive skill quantification are based on the combined time series. Bias correction is an unavoidable topic for decadal predictions due to initial shock, which varies with lead time. Therefore, Boer et al. (2016) recommends leadtime-dependent bias correction.

The predictive skill is quantified by the anomaly correlation coefficient, the anomalies are calculated by removing the respective climatological mean state. In that sense, the climatological mean bias is removed and the coherence reflects the multi-year variations that we evaluate the predictions. The spatial pattern of climatological mean ocean net primary production and phosphate nutrient concentration are shown in Fig. A2 in comparing with the respective observations. Here the climatological mean state is based on the ensemble mean of the focus time period, 1970-2018 for Figs. 1-6 and the last 10 years for Figs. 7-8. We exclude the first 12 years, i.e., 1958-1969, from the analyses and focus on the period from 1970-2018, because the assimilation in the first decade is affected by model adjustment. For the atmospheric CO_2 concentration, which has high correlations close to 1 with observations because of the coherent linear trends, we have also added the root mean square error (RMSE) metric to investigate the added value of assimilation and initialization. In this study, the significance of the predictive skill is tested with a nonparametric bootstrap approach (Goddard et al., 2013). The analyses are based on annual mean data with focus on the frequency of interannual to multi-year variations.

3 Reconstruction of the global carbon budget

By incorporating observational signals, the assimilation simulation from the decadal prediction system based on MPI-ESM captures the evolution of the global carbon budget as well as the climate in observations. The time series from the MPI-ESM assimilation simulation in comparison to the data and suite of simulations from the GCB2019 are shown in Fig.2.

The CO_2 emissions from fossil fuel and industry are in general consistent but with a slight difference in the 1960-1990s between the assimilation simulation (which uses the CO_2 emission forcing provided by CMIP6 for historical and SSP2-4.5 simulations) and GCB2019. This highlights the uncertainty in the CO_2 forcing, which affects the amplitude of the atmospheric CO_2 concentration as it is a cumulative quantity. Cumulatively, the CMIP6 CO_2 emission forcing is 8.20 PgC higher than that from the GCB2019, which results in a difference of atmospheric CO_2 of 3.86 ppm (by dividing a factor of 2.124 PgC $ppm^{-}1$ globally (Ballantyne et al., 2012)). This discrepancy of CO_2 emission might explain to some extent that the simulated atmospheric CO_2 concentration is few ppm higher than the NOAA_GML observations (Dlugokencky and Tans, 2020) (Fig. A3). However, this little difference of a few ppm in atmospheric CO_2 concentration magnitude doesn't noticeably affect the variations in the CO_2 fluxes and the corresponding atmospheric carbon increment (see Fig. 2D-F).

The land-use change induced emissions diagnosed by CBALONE are within the range of GCB2019 multi-model (including JSBACH) simulations from Dynamic Global Vegetation Models (DGVMs) (Fig.2B). The estimates from bookkeeping models show smaller variations than those produced by the DGVMs. Note that the GCBs use the bookkeeping approach for the land-use emissions term. Bookkeeping implies that carbon fluxes are determined from area changes in vegetation types of different vegetation and soil carbon densities, with specific response curves characterizing the evolution of decay and recovery. Carbon densities may stem from recent observations or models, but are kept fixed, i.e. changes in environmental conditions are not

https://doi.org/10.5194/esd-2022-37
Preprint. Discussion started: 1 August 2022

Earth System Dynamics
Discussions

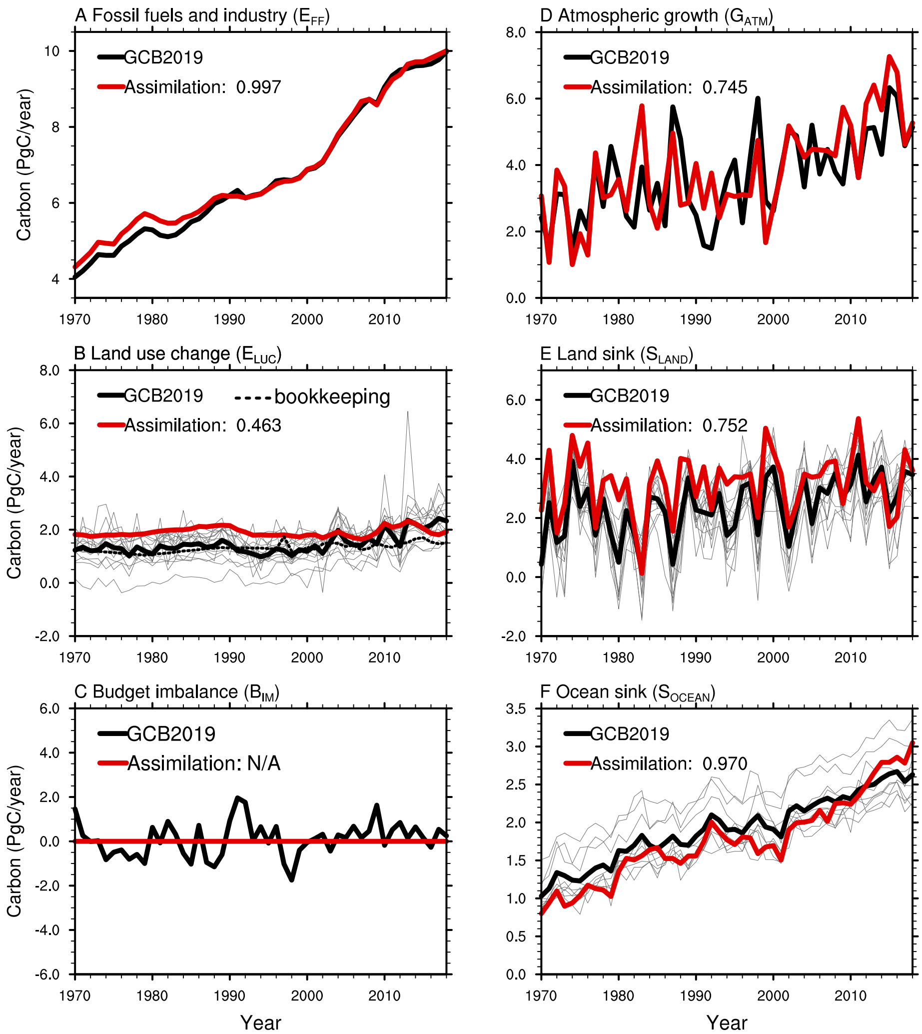

Figure 2. Time series of (A) fossil fuel and industry CO_2 emissions (E_{FF}), (B) emissions from land-use change (E_{LUC}), (C) the budget imbalance (B_{IM}) that is not accounted for by the other terms, (D) atmospheric carbon growth rate (G_{ATM}), (E) the natural terrestrial carbon fluxes (S_{LAND}), and (F) air-sea CO_2 fluxes (S_{OCEAN}) from MPI-ESM1.2-LR assimilation in comparison with Global Carbon Budget (GCB 2019, (Friedlingstein et al., 2019)). Emissions (A & B) are positive when they are fluxes into the atmosphere, while sinks (D, E & F) are positive as fluxes into the respective compartment. A positive B_{IM} means a higher sum of emissions than sinks. The thin grey curves in B, E, and F show individual GCB stand-alone model results. The numbers in the legend show the correlation coefficients between assimilation and GCB2019.

https://doi.org/10.5194/esd-2022-37
Preprint. Discussion started: 1 August 2022

accounted for. The DGVMs by contrast (which are used to provide only an uncertainty range around the bookkeeping models in the GCBs) calculate land-use emissions under transient environmental conditions. This implies first that interannual variability in bookkeeping models is only driven by land-use change, not further interactions with climate variability, which makes the DGVM estimates in general more variable from year to year than the bookkeeping estimates are. Second, it implies that the DGVM-based land-use emissions estimates include the so-called "loss of additional sink capacity" (Pongratz et al., 2014), which refers to the carbon that could have been stored in forests additionally over the course of history (e.g., due to the "CO_2-fertilization" effect) if these forests had not been cleared by expansion of agriculture and forestry. This loss of additionally sink capacity generally increases over time and amounts to about 40% (0.8±0.3 PgC yr^{-1}) over 2009-2018 (Obermeier et al., 2021). This explains why DGVM estimates in Fig. 2B show higher emissions than bookkeeping estimates in recent decades. The DGVM- and expert-based uncertainty range around the GCB bookkeeping estimates is large and MPI-ESM-based land-use change emission estimates have been found to be at the high end of the GCB for all decades by Loughran et al. (2021), consistent with our findings.

By design of the Global Carbon Budget, there is a budget imbalance term because the individual budget terms originate from separate measurements together with stand-alone ocean and land model simulations (Friedlingstein et al., 2019). In this study, we assimilate data products in each sub-models within a fully coupled ESM that considers their interactions. The assimilation ensures evolution of the carbon cycle and climate towards the real world, and in contrast to the GCB, the budget is closed within the Earth system, i.e., no budget imbalance occurs by design (Fig. 2C). Therefore, it is more consistent to attribute the GCB variations using the assimilation simulation based on a fully coupled ESM. The advantage of the current way of Global Carbon Project in assessing GCBs (Friedlingstein et al., 2019) ensures the atmospheric CO_2 directly from measurements, so far ESM-based assimilation requires further efforts in improving the constraint of atmospheric CO_2 from observations.

Atmospheric carbon growth rate and carbon fluxes are reasonably well reproduced in emission-driven assimilation with prognostic atmospheric CO_2 (Fig. 2D-F). The atmospheric carbon growth and the land carbon sink show more pronounced variations on interannual time scales, however, the ocean carbon sink has more pronounced variations on decadal time scales. These variations are captured in the assimilation with high correlations between the assimilation and the GCB2019 of 075, 0.75, and 0.97 for atmospheric growth, land sink, and ocean sink, respectively.

The spatial distribution of climatological mean CO_2 fluxes, the variability as standard deviation, and the coherence in carbon fluxes between GCB2019 and the MPI-ESM reconstruction are shown in Fig. 3. The mean states show a CO_2 influx into the ocean and land in the mid- to high-latitudes and outgassing into the atmosphere in the tropical areas especially over the tropical Pacific (Fig. 3A-B). The variability of CO_2 over land is larger than that over ocean; and the magnitude of variability is larger in the assimilation simulation than in the GCB2019 (Fig. 3C-D). This is expected as the GCB2019 is a multi-model mean estimate and therefore smooths out part of high frequency variability. The correlation of CO_2 fluxes between the reconstruction and GCB2019 is high, especially over the ocean (Fig. 3E). The root mean square deviation (RMSD) scales with the magnitude of carbon fluxes, i.e., with greater values on land than over ocean (Fig. 3F). The large RMSD is partially due to smoothed magnitude of fluxes in GCB2019 from the multi-model mean and also the differences in climatology state for GCB2019 and reconstruction, as shown in Fig. 2E-F.

https://doi.org/10.5194/esd-2022-37
Preprint. Discussion started: 1 August 2022

Earth System Dynamics
Open Access
Discussions

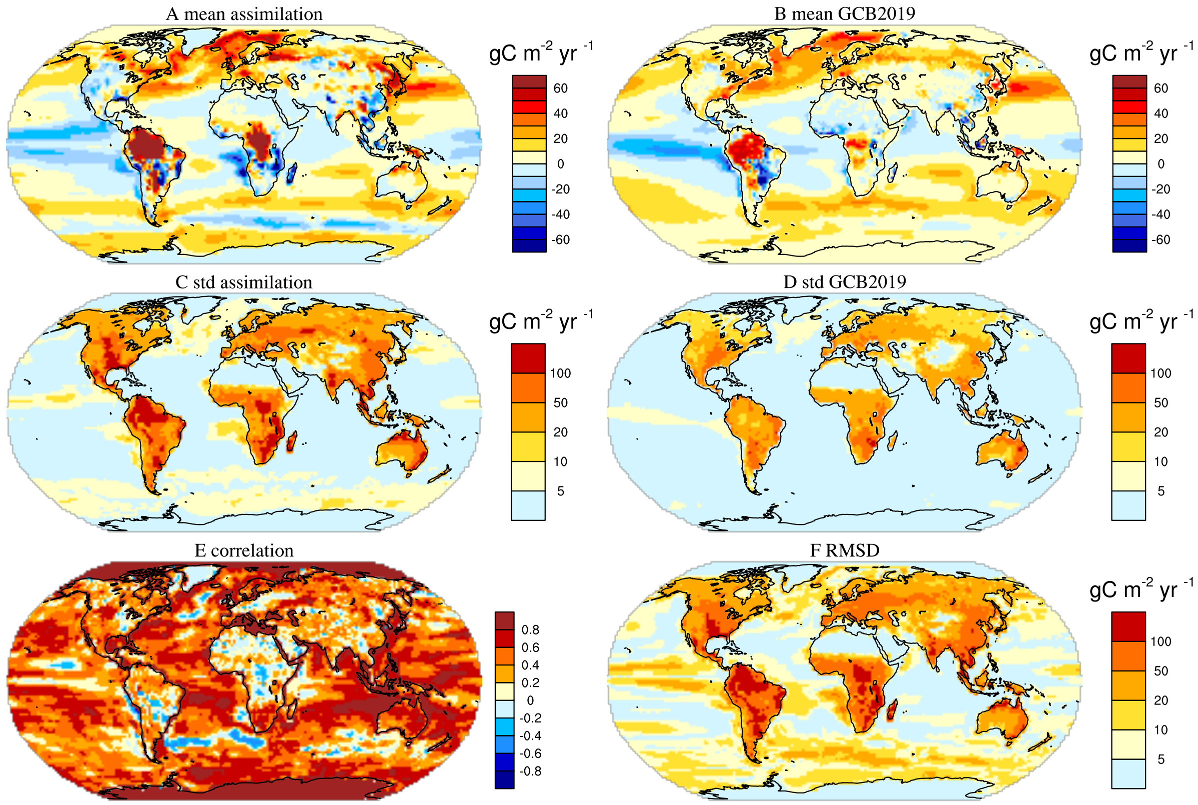

Figure 3. Spatial distribution of the CO_2 fluxes from model assimilations comparing to GCB2019. Climatological mean CO_2 fluxes into the land and the ocean from atmosphere in reconstruction (A) and Global Carbon Budget (GCB 2019 (Friedlingstein et al., 2019)) (B). Temporal variability, i.e., standard deviation, of CO_2 fluxes reconstruction (C) and GCB2019 (D). Correlation and root mean square difference between reconstruction and GCB2019 are shown in E and F. The results are based on annual mean data for the time period from 1970-2018. Positive values in A-D refer to CO_2 fluxes into the ocean or the land.

In general, the historical GCB is well reproduced by the MPI-ESM with assimilating observational products, which enables quantification of the GCB within a closed Earth system, showing that prediction systems provide internally-consistent estimates of the ocean and land carbon sink and serve as an additional line of evidence for the GCB in the future.

4 Predictability of global carbon budget

The initialized predictions start from the assimilation states which are close to observations. Therefore, the information of the observations are incorporated into the prediction system as initial states, which enables the evolution of the global carbon cycle and climate to follow the trajectory of the observations until the predictability horizon is reached.

https://doi.org/10.5194/esd-2022-37
Preprint. Discussion started: 1 August 2022

Earth System Dynamics
Discussions

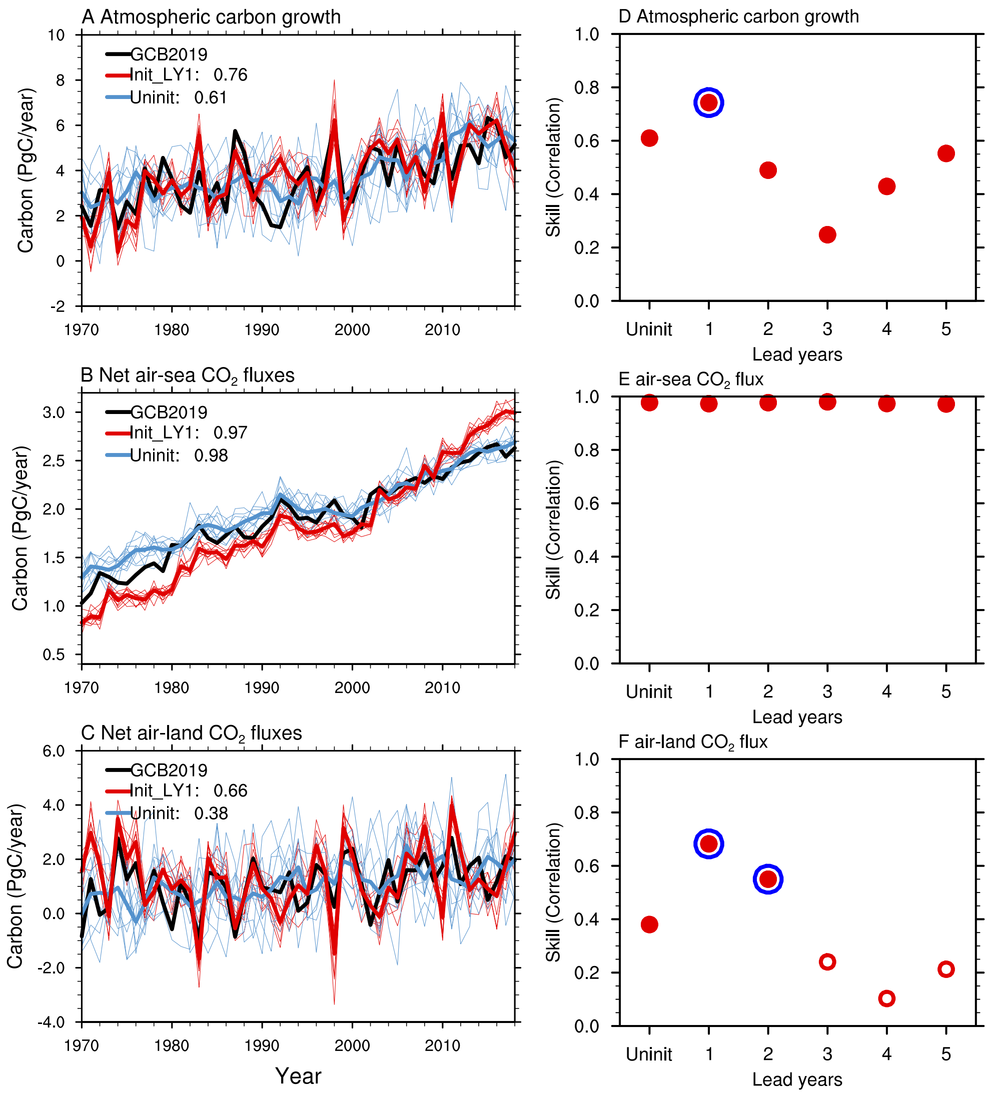

Figure 4. Left panels: Time series of initialized simulations at lead time of 1 year in atmospheric carbon growth rate, i.e., G_{ATM} (A), net air-sea CO_2 fluxes, i.e., S_{OCEAN} (B), and net air-land CO_2 fluxes, i.e., E_{LUC}+S_{LAND} (C) together with Global Carbon Budget (GCB 2019, Friedlingstein et al. (2019)). Positive values in B-C refer to CO_2 fluxes into the ocean or the land. The numbers in the legend show the correlation coefficients between the simulations and GCB2019, the ensemble mean data is used for the calculation. Right panels: Predictive skill of atmospheric carbon growth rate, i.e., G_{ATM} (D), air-sea CO_2 fluxes, i.e., S_{OCEAN} (E), and net air-land CO_2 fluxes, i.e., E_{LUC}+S_{LAND} (F) reference to Global Carbon Budget (GCB 2019, (Friedlingstein et al., 2019)). The filled red circles on top of the open red circles show that the predictive skill is significant at 95% confidence level and the additional larger blue circles indicate improved significant predictive skill due to initialization in comparison to the uninitialized simulations. We use a nonparametric bootstrap approach (Goddard et al., 2013) to assess the significance of predictive skill. The results are based on annual mean data for the time period from 1970-2018.

https://doi.org/10.5194/esd-2022-37
Preprint. Discussion started: 1 August 2022

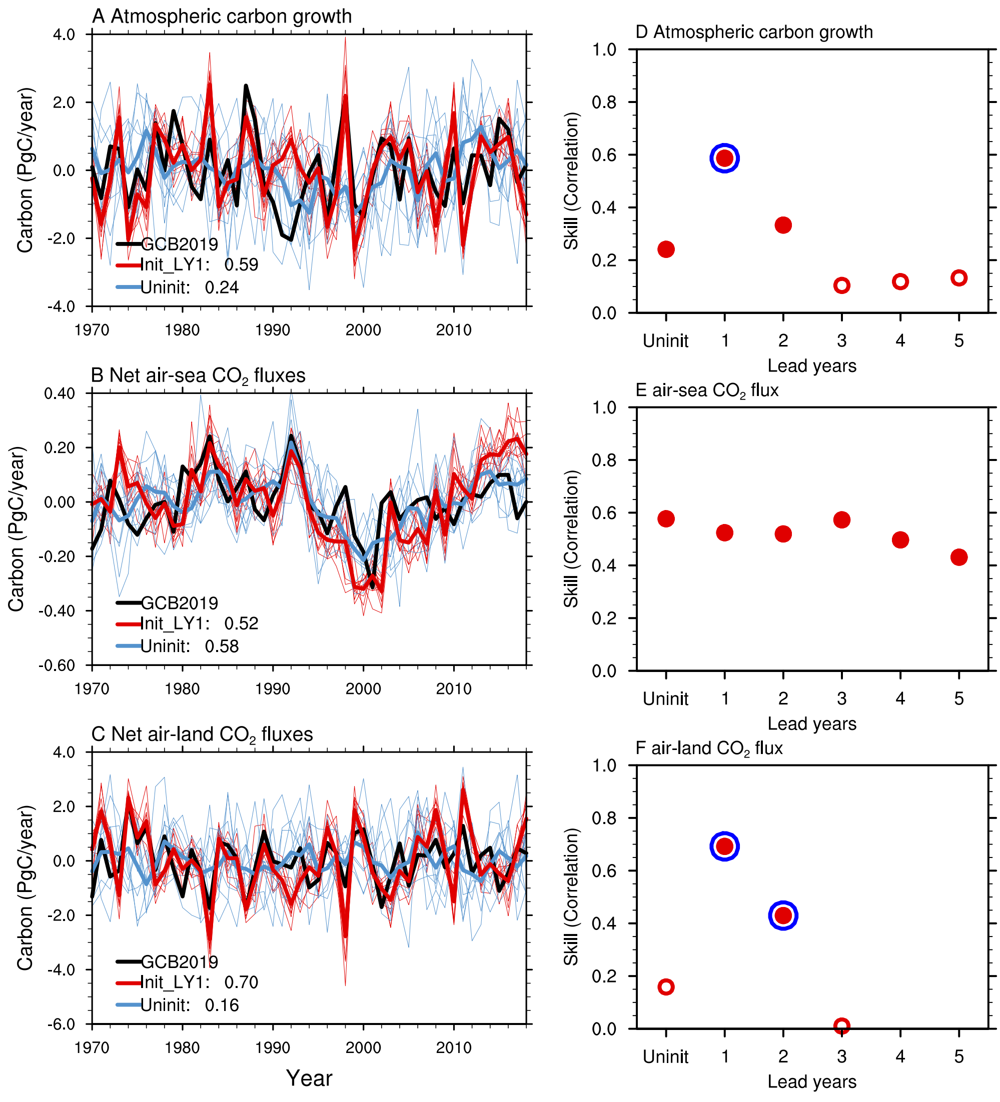

Figure 5. The same as Fig. 4, but with linearly detrended time series.

https://doi.org/10.5194/esd-2022-37
Preprint. Discussion started: 1 August 2022

Earth System Dynamics
Discussions

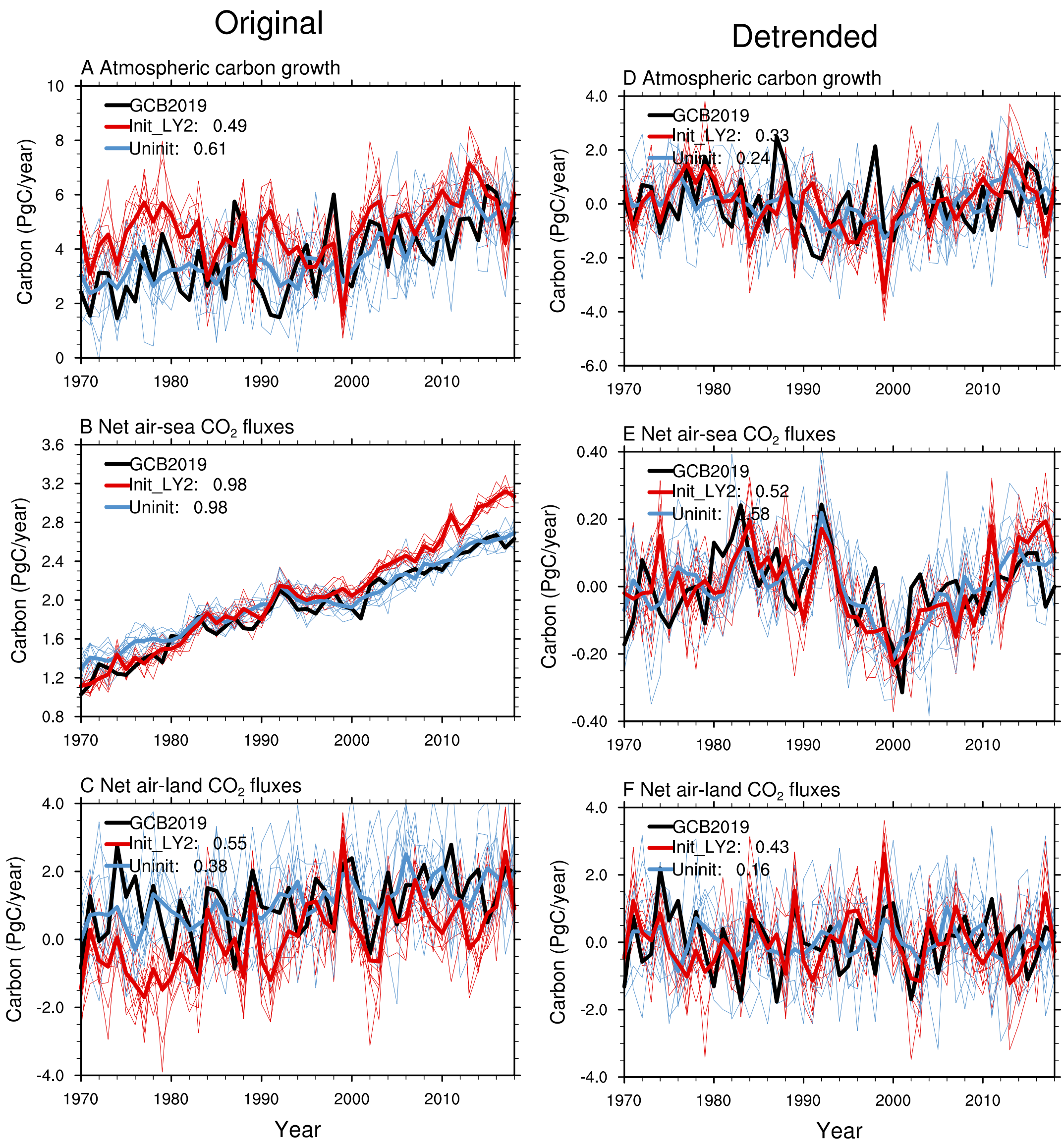

Figure 6. Left panels: Time series of initialized simulations at lead time of 2 years in atmospheric carbon growth rate, i.e., G_{ATM} (A), net air-sea CO_2 fluxes, i.e., S_{OCEAN} (B) and net air-land CO_2 fluxes, i.e., E_{LUC}+S_{LAND} (C) together with Global Carbon Budget (GCB 2019, (Friedlingstein et al., 2019)). Right panels: the same as the left panels, but for linearly detrended time series. The shown time series are based on annual mean data for the time period from 1970-2018. Positive values in B-C and E-F refer to CO_2 fluxes into the ocean or land. The numbers in the legend show the correlation coefficients between the simulations and GCB2019, the ensemble mean data is used for the calculation.

https://doi.org/10.5194/esd-2022-37
Preprint. Discussion started: 1 August 2022

To support the Global Carbon Project in predicting the next-year's GCB one year in advance, we also investigate the predictability focusing on the model hindcasts at lead time of 1 year. As shown in Fig. 4 and Fig. 5, the initialized simulations at lead time of 1 year show high correlations with the GCB2019. The correlations of global atmospheric CO_2 growth, net air-sea CO_2 fluxes and net air-land CO_2 fluxes are 0.59, 0.52, 0.70 after removing the linear trends (Fig. 5 left panels); the correlation of original time series are 0.76, 0.97, and 0.66 (Fig. 4 left panels). The initialized simulations at lead time of 2 years still resemble the variations in the GCB2019 with correlations of 0.49 and higher (Fig. 6 left panels), the detrended time series also show higher correlations than the detrended uninitialized simulations, showing that internal variability can be constrained by initialization (Fig. 6 right panels). As for atmospheric carbon growth, the initialized simulations at lead time of 2 years show coherent interannual variations even with a smaller correlation (0.49) than that of the historical freely evolving run (0.61), which is mainly contributed by the coherent trends of the freely evolving run and the GCB2019. After detrending, the correlations are higher in the initialized simulations than in the uninitialized simulations (comparing Fig. 6 A and D).

The initialized and uninitialized simulations show a comparably good match to GCB2019 with respect to net carbon flux into the ocean (with high correlation up to 0.98) (Fig. 4B), it suggests the good representation of the ocean carbon sink variations (especially on decadal time-scale) in the historical freely evolving uninitialized run. This implies that these variations of the globally integrated ocean carbon sink are more from external forcing rather than internal variability as found in McKinley et al. (2020).

The net carbon flux into the land shows higher correlation for initialized simulations at lead time of 2 years than that for uninitialized simulations (Fig. 4F and Fig. 5F). This indicates the interannual variations are better captured in the initialized model system even after 2 years of free integration. This result implies a predictability of the air-land CO_2 flux of 2 years. The air-land CO_2 fluxes are regulated by the El Niño-Southern Oscillation (ENSO) variations (Loughran et al., 2021; Dunkl et al., 2021), the poor skill in predicting ENSO limits the predictability of the air-land CO_2 fluxes. However, the predictive skill of air-land CO_2 of 2 years is beyond the predictability horizon of ENSO, which is limited to seasonal scale.

We further quantify the predictive skill of the GCB through all the lead time up to 5 years (Fig. 4 right panels and Fig. 5 right panels). The correlation skill relative to GCB2019 is significant for the lead time of 5 years in atmospheric carbon growth and the ocean carbon sink, however, the skill is lower up to 2 years for the air-land CO_2 flux (Fig. 4 D-F). The improved predictive skill of initialized hindcasts compared to the historical uninitialized run is at lead time of 1 year for atmospheric carbon growth and at lead time of 2 years for air-land CO_2 flux. The detrended results (Fig. 5D-F) are similar to those from the original time series. The correlation of atmospheric carbon growth at a lead time of 2 years in the initialized hindcasts are higher than the uninitialized historical run when detrended. This indicates the contribution of a linear trend to the skill of uninitialized historical runs. Although the improvement of predictive skill in the initialized simulation relative to the uninitialized simulation is not significant, the correlations of both initialized simulations at lead time of 2 years and the uninitialized simulations are significantly high as indicated with red solid dots. This suggests the predictability of atmospheric carbon growth in 2 years.

From our MPI-ESM1.2-LR initialized hindcasts, we find that predictive skill of air-sea CO_2 flux is relatively high for up to 5 years, and that of the air-land CO_2 fluxes is up to 2 years. This is consistent with previous studies without an interactive carbon cycle (Ilyina et al., 2021; Lovenduski et al., 2019a, b). Here we extend the prediction system into emission-driven simulations

https://doi.org/10.5194/esd-2022-37
Preprint. Discussion started: 1 August 2022

Earth System Dynamics Discussions

enabling prognostic CO_2 and preserving features of predictability. Furthermore, the prognostic CO_2 from the novel emission-driven decadal prediction system suggests predictability as well, and the atmospheric CO_2 growth rate shows predictive skill
240 of 2 years in the initialized predictions.

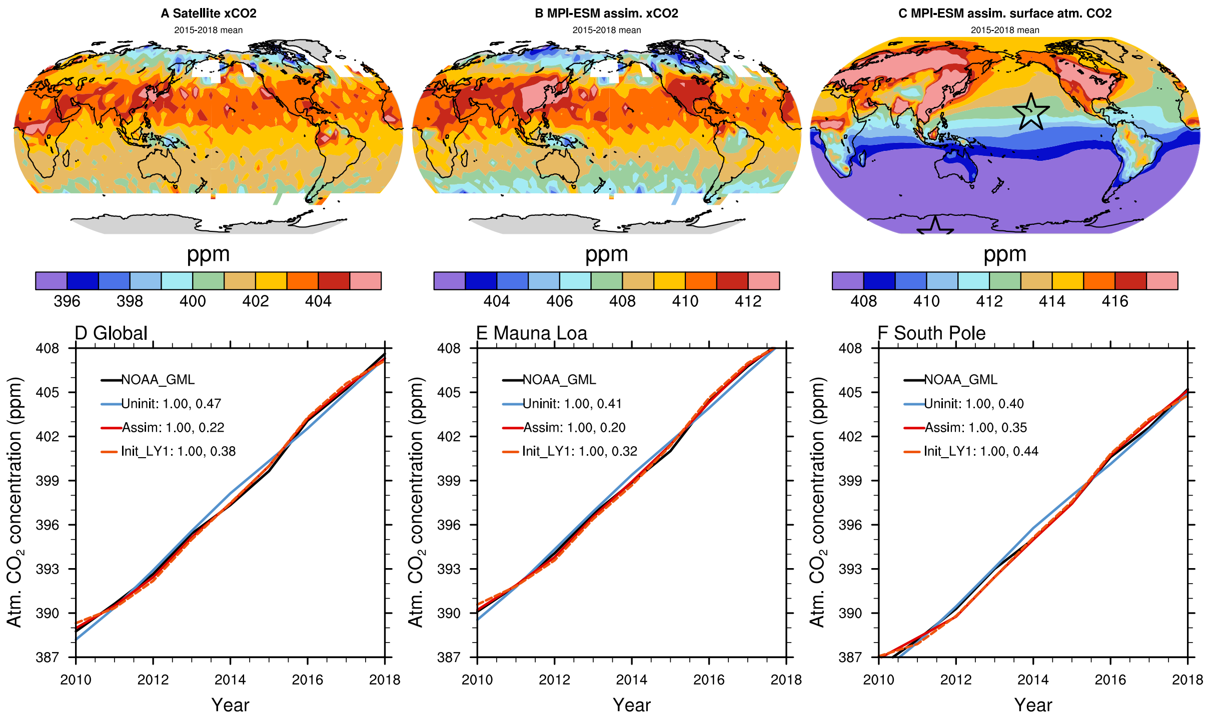

Figure 7. Upper panels: Spatial distribution of 2015-2018 mean satellite-based Obs4MIPs XCO_2 (A) and model assimilation of XCO_2 (resampled according to satellite data availability) (B) and model assimilation of atmospheric CO_2 concentration at 1000hPa level (C). We take a short time period of 2015-2018 because of the limited coverage of satellite data. The satellite XCO_2 data product is from the Climate Data Store Copernicus Climate Change Service (Reuter et al., 2013). The conversion of model simulated CO_2 to XCO_2 is according to Gier et al. (2020) Appendix A. Lower panels: Atmospheric CO_2 concentration in global (D), Mauna Loa (E), and South Pole (F) from the uninitialized (Uninit), assimilation (Assim) simulations, and initialized simulations at lead time of 1 year (Init_LY1) in comparing with observations in the last decade. The location of Mauna Loa and South Pole is shown in panel (C). The numbers in the figure legend show the correlation (left) and root mean square error (RMSE, right) of the simulations relative to observational data from NOAA_GML (Dlugokencky and Tans, 2020). The time series are bias corrected by removing the difference of mean states and linear trend between observation and simulations according to Boer et al. (2016).

5 Atmospheric CO_2 concentration

Fig. 7 shows spatial pattern and time series of atmospheric CO_2 concentration from MPI-ESM simulations together with the satellite XCO_2 and NOAA_GML observations for the last couple years. The XCO_2 from model assimilation (Fig. 7B)

https://doi.org/10.5194/esd-2022-37
Preprint. Discussion started: 1 August 2022

Earth System Dynamics
Discussions

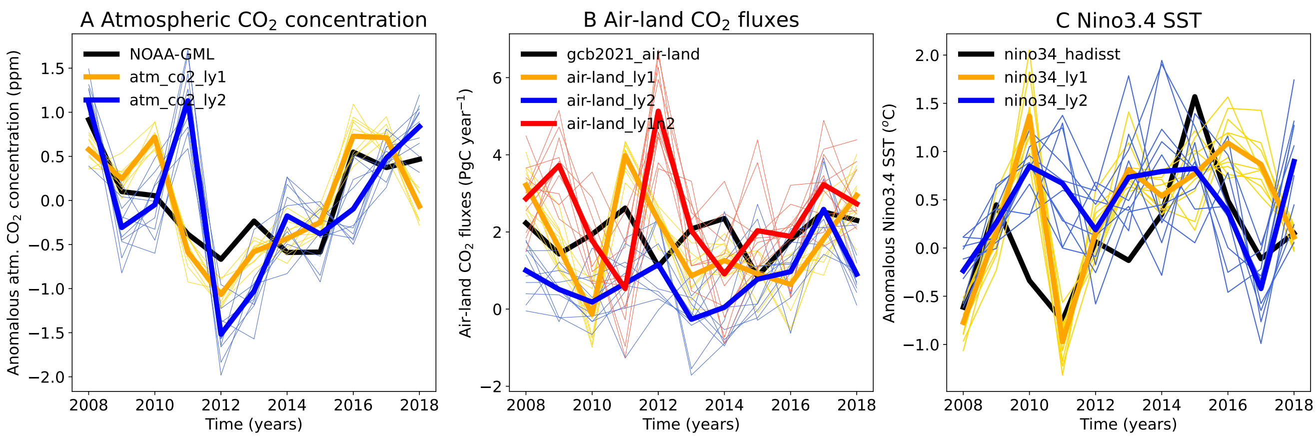

Figure 8. A: Time series of atmospheric CO_2 concentration from initialized simulations at lead time of 1 year and 2 years together with NOAA_GML observation (Dlugokencky and Tans, 2020) in the last 10 years; the time series are detrended and with climatological mean removed. B: Time series of CO_2 fluxes from initialized simulations at lead time of 1 year and 2 years and from GCB2019; The red curves present sum of prediction at lead time of 2 years and the previous year of prediction at lead of 1 year (air-land_ly1n2). C: Time series of nino3.4 SST from model simulations and HadISST. The time series are original model outputs and concatenated according to the lead time of years.

shows the spatial distribution of atmospheric CO_2 concentration which is close to the satellite XCO_2 (Fig. 7A). High CO_2 concentration is found in the tropical to middle latitude of the northern hemisphere. Relatively low CO_2 concentration is in the southern hemisphere and the polar regions. Note the model simulation is several ppm higher than the satellite data, this deviation can be attributed back to the uninitialized historical simulation (see Fig. A3), and the satellite data does not cover all the seasons in high latitudes therefore the sampled model assimilation also represents more summer season XCO_2 there. The surface level CO_2 shows more dominant higher concentration in the northern hemisphere than in the southern hemisphere (Fig. 7C). Here we also the surface atmospheric CO_2 concentration to compare with the measurements in stations Mauna Loa and the South Pole (locations are shown in the figure with stars).

As the atmospheric CO_2 concentration is an accumulative quantity and shows mainly a linear increasing trend, it is necessary to zoom in to visualize the trend slope changes. In addition, the deviation of model simulated atmospheric CO_2 relative to observations in the previous period is accumulated along with the integration of the model, therefore, it ends up with around 8ppm higher global atmospheric CO_2 concentration in the model simulation than in the observations (see Fig. A4). The NOAA_GML data represents the average of atmospheric CO_2 over marine surface sites (Dlugokencky and Tans, 2020), they are slightly smaller than the values on land since the anthropogenic CO_2 emissions are mainly on land. The time series shown in Fig. 7D-F are bias corrected by removing the difference of mean states and linear trends between observation and simulations according to Boer et al. (2016).

The shown atmospheric CO_2 concentration from assimilation follows the evolution of NOAA_GML observation well, with RMSE of 0.22 ppm which is better than the uninitialized historical run with RMSE of 0.72 ppm (Fig. 7D). The initialized simulations could represent the observed evolution well even at lead time of 5 years, with lower RMSE of 0.46 ppm than uninitialized historical run (Fig. A5 and A6). In general, the RMSE increases from lead time of 1 year to 2 years and decreases until lead time of 5 years in both global and observatory sites as Mauna Loa and South Pole (Fig. A5 and A6). The relatively low predictive skill at lead time of 2 years in atmospheric CO_2 concentration is because the model failed to predict the neutral ENSO events in 2010 and La Niña in 2011, and in stead predicts strong El Niño in both years (Fig. 8C). The corresponding air-land CO_2 fluxes are reversed, i.e., the land takes up less CO_2 than expected (Fig. 8B blue solid curve and black solid curve). As the atmospheric CO_2 concentration is a cumulative quantity, the magnitude of interannual variations might be affected by the last several years. We also present the cumulative air-land CO_2 fluxes of the 1st and 2nd year prediction (see the red curves in Fig. 8B), the variations in cumulative air-land CO_2 fluxes are reverse to those in atmospheric CO_2 concentration changes at lead time of 2 years as shown in Fig. 8A blue curves. The results indicate that the air-land CO_2 flux and corresponding atmospheric CO_2 has predictive skill, though the skill at lead time of 2 years is intervened by the predictability of ENSO in some starting year predictions.

This retrospective prediction demonstrates the ability of ESM-based decadal prediction system in reconstructing and predicting the global carbon cycle, with only assimilating the physical atmosphere and ocean fields. As presented in Fig. 5 right panels, the hindcasts also show predictive skill of 5 years for air-sea CO_2 fluxes and 2 years for air-land CO_2 fluxes and atmospheric carbon growth. Hence the confidence of using the ESMs to predict the next year's global carbon budget is high.

6 Conclusions

For the first time, we extend a decadal prediction system based on MPI-ESM to integrate the interactive carbon cycle, driven by fossil fuel emissions, and hence enabling prognostic atmospheric CO_2 predictions. This new setup of assimilation and initialized predictions has one more degree of freedom, i.e., enabling prognostic atmospheric CO_2 and the corresponding interactive effects, and represents the global carbon cycle closer to observations.

The variations of atmospheric carbon growth rate and CO_2 fluxes among atmosphere, ocean, and land are well reconstructed in our assimilation simulations, with high correlations (0.75, 0.97, and 0.75) with the GCB2019. This enables a closed quantification of the GCB within an Earth system model. Furthermore, our reconstruction of the GCB provides an additional line of evidence for quantifying the annual GCB and opens new opportunities in assessing the efficiency of carbon sinks and internally consistent metrics. In particular, this approach eliminates the budget imbalance term that arises in GCBs of the Gobal Carbon Project due to the combination of various, not fully consistent model and data approaches.

To further support the Global Carbon Project in predicting next year GCB, the focus of the predictability investigation are on the lead time of 1 year. The results show high confidence of predicting the global carbon budget in the next year with the MPI-ESM prediction system. We further demonstrate that retrospective predictions of the global carbon budget have predictive skill for up to 5 years for air-sea CO_2 fluxes and up to 2 years for air-land fluxes and atmospheric carbon growth rate. This

https://doi.org/10.5194/esd-2022-37
Preprint. Discussion started: 1 August 2022

Earth System Dynamics
Discussions

means that the variations of atmospheric CO_2 are better reproduced in the assimilation and retrospective predictions than in the uninitialized freely evolving historical simulations.

We preserve the high predictive power of the prediction system when transferred to an emission-driven configuration, simulating the atmospheric CO_2 with reasonable accuracy. But the emission-driven decadal prediction system delivers the huge advantage of simulating the land and ocean fluxes in response to fossil-fuel and land-use change emissions, including all feedbacks. Further efforts towards increasing observations to initialize the ESMs, assess the predictive skill, and provide reliable global estimated and spatial distribution of anthropogenic and natural emissions, will lead to more reliable reconstruction and predictions. This study is based on single model simulations, further multi-model simulations will alleviate dependence of individual model responses and hence demonstrate robust changes of the global carbon cycle.

We demonstrate that our emission-driven decadal prediction system shows capability to reconstruct and predict the GCB and atmospheric CO_2 concentration variations. This will be a powerful tool in supporting the global carbon stocktaking and informing policies that comply with the goals of the Paris Agreement.

Code and data availability. Primary data and scripts used in the analysis that may be useful in reproducing the authors' work are archived by the Max Planck Institute for Meteorology and can be obtained via the institutional repository http://hdl.handle.net/21.11116/0000-0009-6B84-A.

Author contributions. H.L. and T.I. conceived the idea. H.L. designed this study, ran the MPI-ESM simulations, performed the analyses, and drafted the manuscript. T.L. ran the CBALONE module simulations. T.I., T.L., A.S., and J.P. contributed in discussing the results and editing the manuscript.

https://doi.org/10.5194/esd-2022-37
Preprint. Discussion started: 1 August 2022

Earth System Dynamics
Discussions

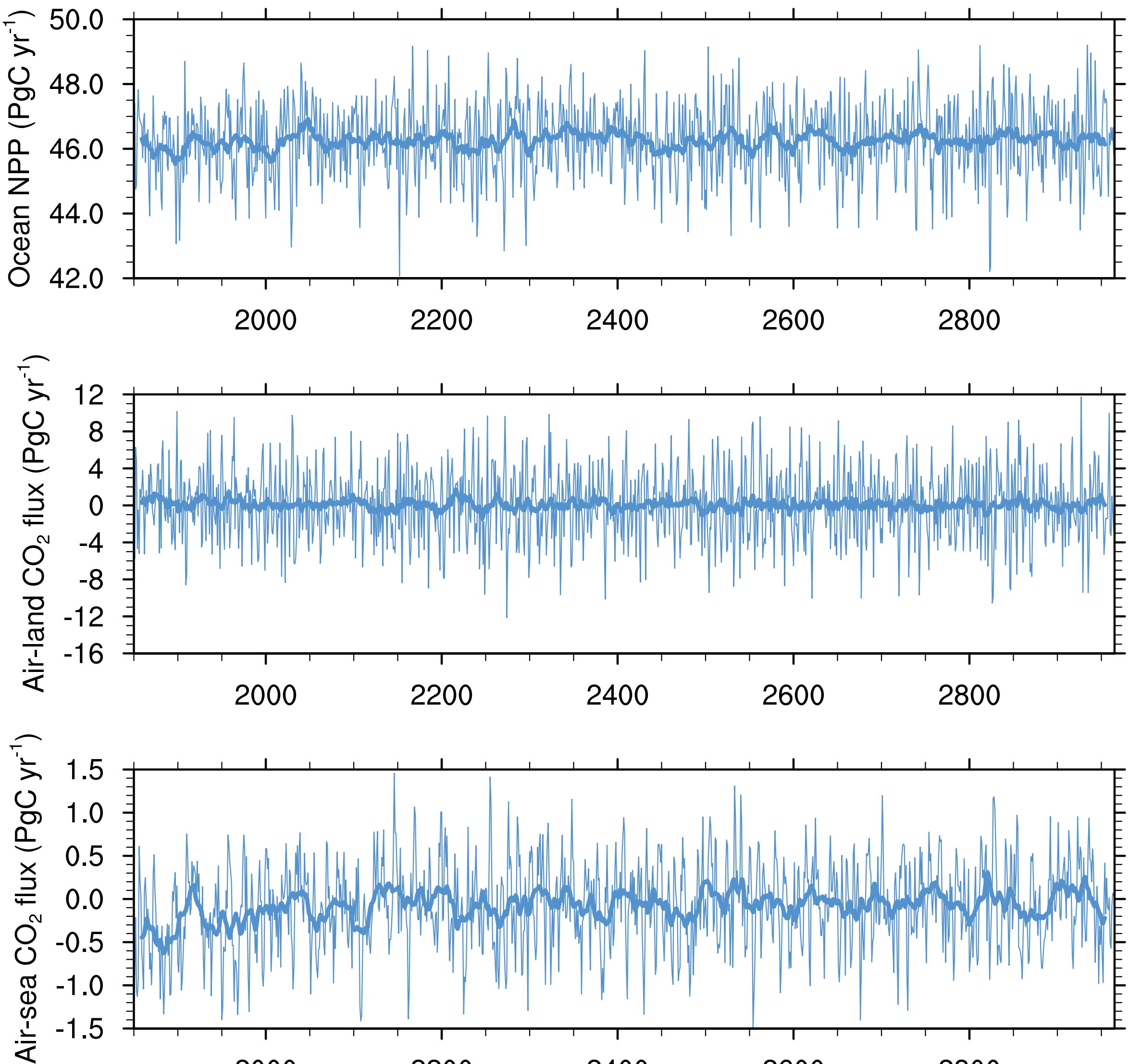

Figure A1. Time series of model simulations of ocean net primary production, air-sea CO2 flux and air-land CO2 flux in the pre-industrial control run. The thin lines are annual mean time series, and the thick lines are 20-year running mean time series.

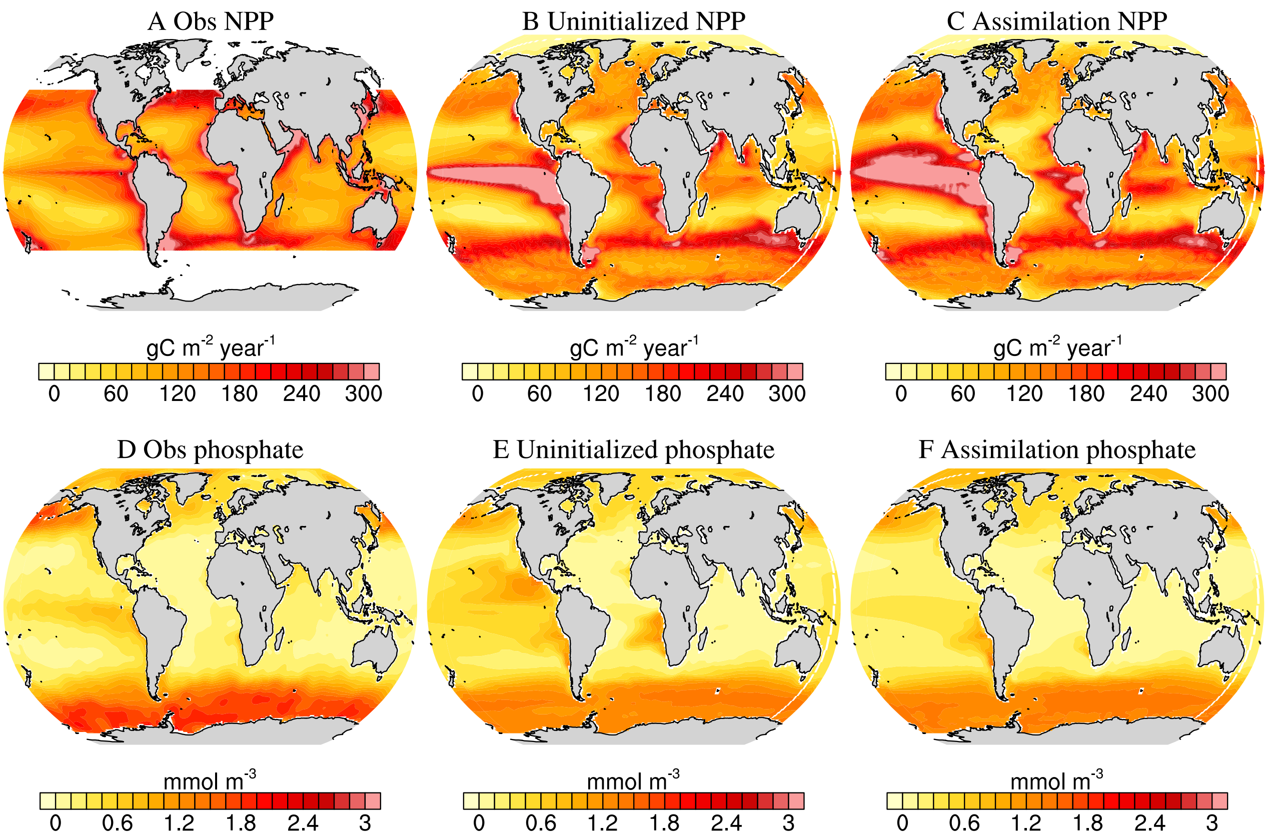

Figure A2. Climatological mean of ocean net primary production (NPP) and phosphate concentration from observation and from model simulations. NPP observational reference data are estimated from ocean color measurements obtained by the Sea-viewing Wide Field-of-view Sensor (SeaWiFS) instrument of the OrbView-2 satellite for September 1997 to December 2002 and the Moderate Resolution Imaging Spectroradiometer (MODIS) of the Aqua satellite from 2003 to 2014 ((Behrenfeld and Falkowski, 1997), http://science.oregonstate.edu/ocean.productivity/index.php). Phosphate observations are from the World Ocean Atlas 2018 (Garcia et al., 2019). The corresponding NPP data from models are 1998-2017 mean and phosphate data are from 1970-2018 mean.

https://doi.org/10.5194/esd-2022-37
Preprint. Discussion started: 1 August 2022

Earth System Dynamics
Discussions

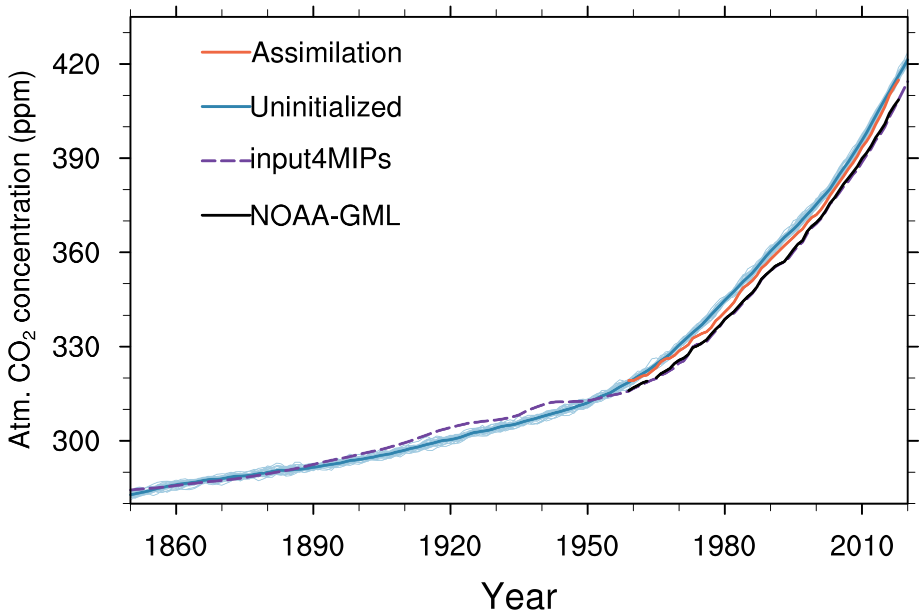

Figure A3. Time series of atmospheric CO_2 concentration from model simulations and observation from 1850-2020. The assimilation and uninitialized simulations are shown with orange and blue solid lines, respectively. The CMIP6 input4MIPs atmospheric CO_2 concentration forcing and the NOAA_GML observation (Dlugokencky and Tans, 2020) are shown with blue dashed line and black solid lines, respectively.

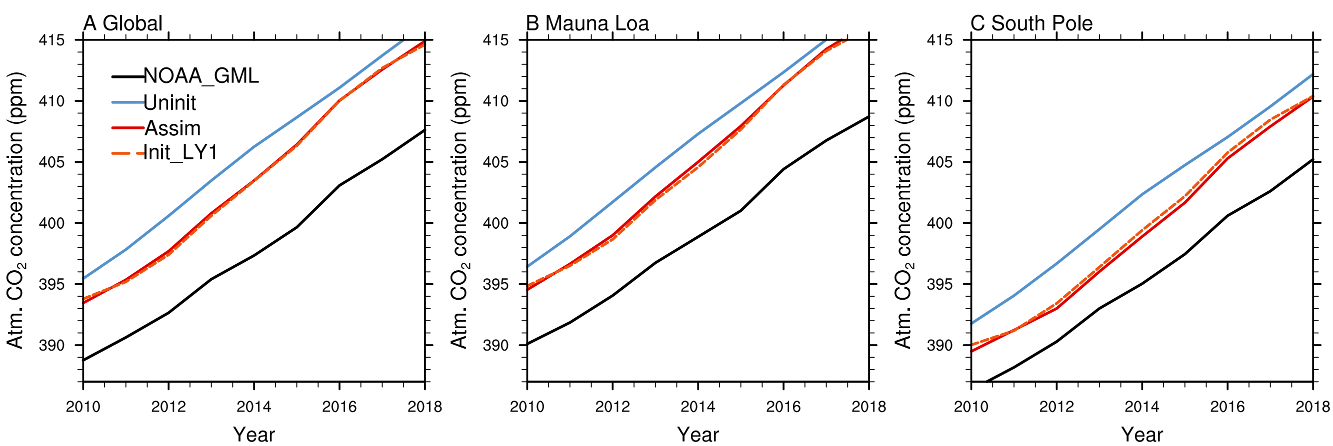

Figure A4. Atmospheric CO_2 concentration from the assimilation and initialized simulations at lead time of 1 year together with NOAA_GML observation (Dlugokencky and Tans, 2020) in the last 10 years. The time series are original model outputs and concatenated according to the lead time of years.

https://doi.org/10.5194/esd-2022-37
Preprint. Discussion started: 1 August 2022

Earth System Dynamics Discussions

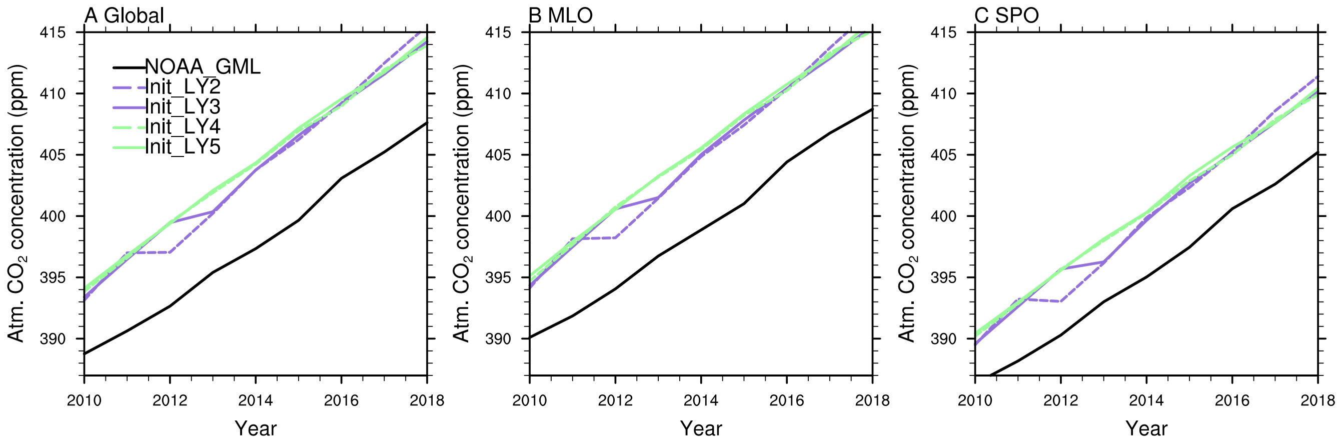

Figure A5. Atmospheric CO_2 concentration from initialized simulations at lead time of 2-5 years together with NOAA_GML observation (Dlugokencky and Tans, 2020) in the last 10 years. The time series are original model outputs and concatenated according to the lead time of years.

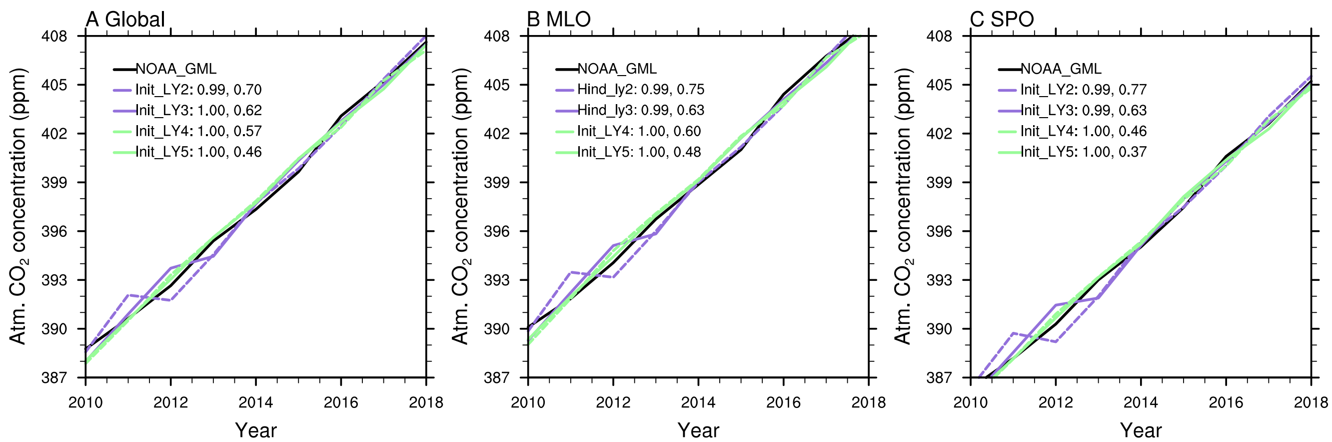

Figure A6. The same as Fig. A5, but with bias corrected mean states and linear trend.

https://doi.org/10.5194/esd-2022-37
Preprint. Discussion started: 1 August 2022

Earth System Dynamics Discussions

S1

Table A1. Simulations based on MPI-ESM1.2-LR. Resolution for Atmosphere: T63L47, Ocean: GR15L40. The design of the prediction simulations is according to previous study (Marotzke et al., 2016; Li et al., 2019). The assimilation starts from the end of year 1958 in an uninitialized simulation. The nudging is strong therefore an assimilation starting from a different uninitialized simulation would end up with similar evolution of the climate and carbon cycle. Fig. 1 illustrates the simulations with evolution of atmospheric CO_2 growth rate together with observation. The initialized simulations start from the assimilation yearly from October 31st and run freely for 2 months plus 5 years afterwards. We have 60 runs for one ensemble of initialized simulations starting from 1960 to 2019 annually and run for 5 years and 2 months each, i.e., Nov. 1960 - Dec. 1965 for starting year 1960, Nov. 1961 - Dec. 1966 for starting year 1961, and so forth until Nov. 2018 - Dec. 2023. The ensembles are generated with lagged 1-day initialization, i.e., the simulations start from 10 consecutive days from October 31st to November 9th. The ensembles for uninitialized simulations (shown as in Fig. A3) are generated by starting from different year of the control simulation (Fig. A1).

Simulations	Ensemble members	Nudging	Initial condition	Time period
Uninitialized	10	N/A	Preindustrial	1850-2099
Assimilation	1	Atm.: ERA Ocean: ORAS4 anomalies (without 5N-5S band) Sea Ice: NSIDC	Uninitialized	1959-2018
Initialized	10	N/A	Assimilation	1960-1965 ... 2018-2023

Competing interests. The authors declare no competing interests.

Acknowledgements. We acknowledge funding from the Federal Ministry of Education and Research in Germany (BMBF) through the research program MiKlip (grant no. 01LP1517B), the European Union's Horizon 2020 research and innovation program under grant agreement no. 641816 (CRESCENDO), the European Union's Horizon 2020 research and innovation program under grant agreement no. 821003 (4C), and the Deutsche Forschungsgemeinschaft (DFG, German Research Foundation) under Germany's Excellence Strategy—EXC 2037 'CLICCS—Climate, Climatic Change, and Society'—Project No.: 390683824, contribution to the Center for Earth System Research and Sustainability (CEN) of Universität Hamburg. We thank Julia Nabel and Jochem Marotzke for internal reviewing this manuscript. We thank Veronika Gayler and Thomas Raddatz for providing script and forcing data for setting up MPI-ESM1.2-LR emission-driven simulations. We thank Yohei Takano for running 4 members of uninitialized simulations and Kameswar Modali for helping set up the assimilation and initialized simulations. We thank Pierre Friedlingstein, Judith Hauck, Stephen Sitch and co-authors for making the global carbon budget data from Global Carbon Project available. This work used resources of the Deutsches Klimarechenzentrum (DKRZ) granted by its Scientific

Steering Committee (WLA) under project ID bm1124.

https://doi.org/10.5194/esd-2022-37
Preprint. Discussion started: 1 August 2022

Earth System Dynamics
Discussions

References

Ballantyne, A. á., Alden, C. á., Miller, J. á., Tans, P. á., and White, J.: Increase in observed net carbon dioxide uptake by land and oceans during the past 50 years, Nature, 488, 70–72, 2012.

Balmaseda, M. A., Mogensen, K., and Weaver, A. T.: Evaluation of the ECMWF ocean reanalysis system ORAS4, Quarterly journal of the royal meteorological society, 139, 1132–1161, 2013.

Bastos, A., O'Sullivan, M., Ciais, P., Makowski, D., Sitch, S., Friedlingstein, P., Chevallier, F., Rödenbeck, C., Pongratz, J., Luijkx, I., et al.: Sources of uncertainty in regional and global terrestrial CO2 exchange estimates, Global Biogeochemical Cycles, 34, e2019GB006 393, 2020.

Behrenfeld, M. J. and Falkowski, P. G.: Photosynthetic rates derived from satellite-based chlorophyll concentration, Limnology and oceanography, 42, 1–20, 1997.

Boer, G. J., Smith, D. M., Cassou, C., Doblas-Reyes, F., Danabasoglu, G., Kirtman, B., Kushnir, Y., Kimoto, M., Meehl, G. A., Msadek, R., et al.: The decadal climate prediction project (DCPP) contribution to CMIP6, Geoscientific Model Development (Online), 9, 2016.

Bunzel, F., Notz, D., Baehr, J., Müller, W. A., and Fröhlich, K.: Seasonal climate forecasts significantly affected by observational uncertainty of Arctic sea ice concentration, Geophysical Research Letters, 43, 852–859, 2016.

Canadell, J. G., Le Quéré, C., Raupach, M. R., Field, C. B., Buitenhuis, E. T., Ciais, P., Conway, T. J., Gillett, N. P., Houghton, R., and Marland, G.: Contributions to accelerating atmospheric CO2 growth from economic activity, carbon intensity, and efficiency of natural sinks, Proceedings of the national academy of sciences, 104, 18 866–18 870, 2007.

Dee, D. P., Uppala, S. M., Simmons, A., Berrisford, P., Poli, P., Kobayashi, S., Andrae, U., Balmaseda, M., Balsamo, G., Bauer, d. P., et al.: The ERA-Interim reanalysis: Configuration and performance of the data assimilation system, Quarterly Journal of the royal meteorological society, 137, 553–597, 2011.

Dlugokencky, E. and Tans, P.: Trends in atmospheric carbon dioxide, National Oceanic and Atmospheric Administration, Global Monitoring Laboratory (NOAA_GML), https://gml.noaa.gov/ccgg/trends/, 2020.

Dunkl, I., Spring, A., Friedlingstein, P., and Brovkin, V.: Process-based analysis of terrestrial carbon flux predictability, Earth System Dynamics, 12, 1413–1426, 2021.

Eyring, V., Bony, S., Meehl, G. A., Senior, C. A., Stevens, B., Stouffer, R. J., and Taylor, K. E.: Overview of the Coupled Model Intercomparison Project Phase 6 (CMIP6) experimental design and organization, Geoscientific Model Development, 9, 1937–1958, 2016.

Fransner, F., Counillon, F., Bethke, I., Tjiputra, J., Samuelsen, A., Nummelin, A., and Olsen, A.: Ocean Biogeochemical PredictionsâInitialization and Limits of Predictability, Frontiers in Marine Science, 7, 386, https://doi.org/10.3389/fmars.2020.00386, 2020.

Friedlingstein, P., Jones, M. W., O'Sullivan, M., Andrew, R. M., Hauck, J., Peters, G. P., Peters, W., Pongratz, J., Sitch, S., Le Quéré, C., Bakker, D. C. E., Canadell, J. G., Ciais, P., Jackson, R. B., Anthoni, P., Barbero, L., Bastos, A., Bastrikov, V., Becker, M., Bopp, L., Buitenhuis, E., Chandra, N., Chevallier, F., Chini, L. P., Currie, K. I., Feely, R. A., Gehlen, M., Gilfillan, D., Gkritzalis, T., Goll, D. S., Gruber, N., Gutekunst, S., Harris, I., Haverd, V., Houghton, R. A., Hurtt, G., Ilyina, T., Jain, A. K., Joetzjer, E., Kaplan, J. O., Kato, E., Klein Goldewijk, K., Korsbakken, J. I., Landschützer, P., Lauvset, S. K., Lefèvre, N., Lenton, A., Lienert, S., Lombardozzi, D., Marland, G., McGuire, P. C., Melton, J. R., Metzl, N., Munro, D. R., Nabel, J. E. M. S., Nakaoka, S.-I., Neill, C., Omar, A. M., Ono, T., Peregon, A., Pierrot, D., Poulter, B., Rehder, G., Resplandy, L., Robertson, E., Rödenbeck, C., Séférian, R., Schwinger, J., Smith, N., Tans, P. P., Tian, H., Tilbrook, B., Tubiello, F. N., van der Werf, G. R., Wiltshire, A. J., and Zaehle, S.: Global Carbon Budget 2019, Earth System Science Data, 11, 1783–1838, https://doi.org/10.5194/essd-11-1783-2019, 2019.

https://doi.org/10.5194/esd-2022-37
Preprint. Discussion started: 1 August 2022

Friedlingstein, P., O'Sullivan, M., Jones, M. W., Andrew, R. M., Hauck, J., Olsen, A., Peters, G. P., Peters, W., Pongratz, J., Sitch, S., et al.: Global carbon budget 2020, Earth System Science Data, 12, 3269–3340, 2020.

Garcia, H., Weathers, K., Paver, C., Smolyar, I., Boyer, T., Locarnini, M., Zweng, M., Mishonov, A., Baranova, O., Seidov, D., et al.: World ocean atlas 2018. Vol. 4: Dissolved inorganic nutrients (phosphate, nitrate and nitrate+ nitrite, silicate), 2019.

Gier, B. K., Buchwitz, M., Reuter, M., Cox, P. M., Friedlingstein, P., and Eyring, V.: Spatially resolved evaluation of earth system models with satellite column-averaged CO 2, Biogeosciences, 17, 6115–6144, 2020.

Goddard, L., Kumar, A., Solomon, A., Smith, D., Boer, G., Gonzalez, P., Kharin, V., Merryfield, W., Deser, C., Mason, S. J., et al.: A verification framework for interannual-to-decadal predictions experiments, Climate Dynamics, 40, 245–272, 2013.

Hansis, E., Davis, S. J., and Pongratz, J.: Relevance of methodological choices for accounting of land use change carbon fluxes, Global Biogeochemical Cycles, 29, 1230–1246, 2015.

Hurtt, G. C., Chini, L., Sahajpal, R., Frolking, S., Bodirsky, B. L., Calvin, K., Doelman, J. C., Fisk, J., Fujimori, S., Klein Goldewijk, K., et al.: Harmonization of global land use change and management for the period 850–2100 (LUH2) for CMIP6, Geoscientific Model Development, 13, 5425–5464, 2020.

Ilyina, T., Six, K. D., Segschneider, J., Maier-Reimer, E., Li, H., and Núñez-Riboni, I.: Global ocean biogeochemistry model HAMOCC: Model architecture and performance as component of the MPI-Earth system model in different CMIP5 experimental realizations, Journal of Advances in Modeling Earth Systems, 5, 287–315, 2013.

Ilyina, T., Li, H., Spring, A., Müller, W. A., Bopp, L., Chikamoto, M. O., Danabasoglu, G., Dobrynin, M., Dunne, J., Fransner, F., et al.: Predictable variations of the carbon sinks and atmospheric CO2 growth in a multi-model framework, Geophysical Research Letters, 48, e2020GL090 695, 2021.

Jones, C. D., Arora, V., Friedlingstein, P., Bopp, L., Brovkin, V., Dunne, J., Graven, H., Hoffman, F., Ilyina, T., John, J. G., et al.: C4MIP–The coupled climate–carbon cycle model intercomparison project: Experimental protocol for CMIP6, Geoscientific Model Development, 9, 2853–2880, 2016.

Landschützer, P., Ilyina, T., and Lovenduski, N. S.: Detecting Regional Modes of Variability in Observation-Based Surface Ocean pCO_2, Geophysical Research Letters, 46, 2670–2679, 2019.

Li, H. and Ilyina, T.: Current and future decadal trends in the oceanic carbon uptake are dominated by internal variability, Geophysical Research Letters, 45, 916–925, 2018.

Li, H., Ilyina, T., Müller, W. A., and Sienz, F.: Decadal predictions of the North Atlantic CO_2 uptake, Nature communications, 7, 1–7, 2016.

Li, H., Ilyina, T., Müller, W. A., and Landschützer, P.: Predicting the variable ocean carbon sink, Science advances, 5, eaav6471, 2019.

Loughran, T. F., Boysen, L., Bastos, A., Hartung, K., Havermann, F., Li, H., Nabel, J. E. M. S., Obermeier, W. A., and Pongratz, J.: Past and future climate variability uncertainties in the global carbon budget using the MPI Grand Ensemble, Global Biogeochemical Cycles, 35, e2021GB007 019, 2021.

Lovenduski, N. S., Bonan, G. B., Yeager, S. G., Lindsay, K., and Lombardozzi, D. L.: High predictability of terrestrial carbon fluxes from an initialized decadal prediction system, Environmental Research Letters, 14, 124 074, 2019a.

Lovenduski, N. S., Yeager, S. G., Lindsay, K., and Long, M. C.: Predicting near-term variability in ocean carbon uptake, Earth System Dynamics (Online), 10, 2019b.

Marotzke, J., Müller, W. A., Vamborg, F. S., Becker, P., Cubasch, U., Feldmann, H., Kaspar, F., Kottmeier, C., Marini, C., Polkova, I., et al.: MiKlip: A national research project on decadal climate prediction, Bulletin of the American Meteorological Society, 97, 2379–2394, 2016.

Marsland, S. J., Haak, H., Jungclaus, J. H., Latif, M., and Röske, F.: The Max-Planck-Institute global ocean/sea ice model with orthogonal curvilinear coordinates, Ocean modelling, 5, 91–127, 2003.

Mauritsen, T., Bader, J., Becker, T., Behrens, J., Bittner, M., Brokopf, R., Brovkin, V., Claussen, M., Crueger, T., Esch, M., et al.: Developments in the MPI-M Earth System Model version 1.2 (MPI-ESM1. 2) and its response to increasing CO_2, Journal of Advances in Modeling Earth Systems, 11, 998–1038, 2019.

McKinley, G. A., Fay, A. R., Eddebbar, Y. A., Gloege, L., and Lovenduski, N. S.: External forcing explains recent decadal variability of the ocean carbon sink, AGU Advances, 1, e2019AV000 149, 2020.

Obermeier, W. A., Nabel, J. E., Loughran, T., Hartung, K., Bastos, A., Havermann, F., Anthoni, P., Arneth, A., Goll, D. S., Lienert, S., et al.: Modelled land use and land cover change emissions–a spatio-temporal comparison of different approaches, Earth System Dynamics, 12, 635–670, 2021.

Park, J.-Y., Stock, C. A., Yang, X., Dunne, J. P., Rosati, A., John, J., and Zhang, S.: Modeling global ocean biogeochemistry with physical data assimilation: a pragmatic solution to the equatorial instability, Journal of Advances in Modeling Earth Systems, 10, 891–906, 2018.

Paulsen, H., Ilyina, T., Six, K. D., and Stemmler, I.: Incorporating a prognostic representation of marine nitrogen fixers into the global ocean biogeochemical model HAMOCC, Journal of Advances in Modeling Earth Systems, 9, 438–464, 2017.

Peters, G. P., Le Quéré, C., Andrew, R. M., Canadell, J. G., Friedlingstein, P., Ilyina, T., Jackson, R. B., Joos, F., Korsbakken, J. I., McKinley, G. A., et al.: Towards real-time verification of CO2 emissions, Nature Climate Change, 7, 848–850, 2017.

Pongratz, J., Reick, C. H., Houghton, R., and House, J.: Terminology as a key uncertainty in net land use and land cover change carbon flux estimates, Earth System Dynamics, 5, 177–195, 2014.

Reick, C. H., Gayler, V., Goll, D., Hagemann, S., Heidkamp, M., Nabel, J. E., Raddatz, T., Roeckner, E., Schnur, R., and Wilkenskjeld, S.: JSBACH 3-The land component of the MPI Earth System Model: documentation of version 3.2, 2021.

Reuter, M., Bösch, H., Bovensmann, H., Bril, A., Buchwitz, M., Butz, A., Burrows, J., O'Dell, C., Guerlet, S., Hasekamp, O., et al.: A joint effort to deliver satellite retrieved atmospheric CO 2 concentrations for surface flux inversions: the ensemble median algorithm EMMA, Atmospheric Chemistry and Physics, 13, 1771–1780, 2013.

Séférian, R., Berthet, S., and Chevallier, M.: Assessing the decadal predictability of land and ocean carbon uptake, Geophysical Research Letters, 45, 2455–2466, 2018.

Spring, A. and Ilyina, T.: Predictability Horizons in the Global Carbon Cycle Inferred From a Perfect-Model Framework, Geophysical Research Letters, 47, e2019GL085 311, 2020.

Spring, A., Ilyina, T., and Marotzke, J.: Inherent uncertainty disguises attribution of reduced atmospheric CO2 growth to CO2 emission reductions for up to a decade, Environmental Research Letters, 15, 114 058, 2020.

Spring, A., Dunkl, I., Li, H., Brovkin, V., and Ilyina, T.: Trivial improvements of predictive skill due to direct reconstruction of global carbon cycle, Earth System Dynamics Discussions, pp. 1–36, 2021.

Uppala, S. M., Kållberg, P., Simmons, A., Andrae, U., Bechtold, V. D. C., Fiorino, M., Gibson, J., Haseler, J., Hernandez, A., Kelly, G., et al.: The ERA-40 re-analysis, Quarterly Journal of the Royal Meteorological Society: A journal of the atmospheric sciences, applied meteorology and physical oceanography, 131, 2961–3012, 2005.